Sliding Singularities of Bounded Invertible Planar Piecewise Isometric Dynamics

Byungik Kahng, Miguel Cuadros and Jonathan Sullivan

***Abstract*—** It is known that the singularities of bounded invertible piecewise isometric dynamical systems in Euclidean plane can be classified as, removable, sliding and shuffling singularities, based upon their geometrical aspects. Moreover, it is known that the Devaney-chaos of the bounded invertible piecewise isometric systems can be generated only from the sliding singularities, while the other singularities remain innocuous. For this reason, we concentrate our efforts on the investigation of the sliding singularity. We begin with re-establishing the distinction between the sliding and shuffling singularities in simpler terms. And then, we calculate the *sliding ratios* explicitly for a class of invertible planar piecewise isometric systems.

***Keywords*—** Devaney-chaos, Piecewise continuous dynamical system, Piecewise isometric dynamical system, Singularity.

I. Introduction

THE study of piecewise isometric dynamical systems, which had once been regarded as an "emerging area" [8], has now established itself as an important branch of mathematics. The applications of piecewise isometric dynamics include, digital signal processing [1], [2], [3], [4], [5], [6], [7], [24], [25], [29], billiards and dual billiards [10], [30], kicked oscillators [26], [27], [28], automatic control systems with singular disturbance [11], [12], [13], [19], just to name a few.

The key component, in fact the only key component, of a piecewise isometric system is its singularity. The piecewise isometric dynamics often generates esthetically beautiful complex orbit structure as visualized in Figure I.1. This is exclusively due to the singularity. Aside from the singularity, a piecewise isometric dynamical system is nothing but a trivial repetition of rotation, inversion or translation. In other words, the piecewise isometric dynamics reveal the contribution of the singularity, which is abundant in nature, without being interfered by other sources of complex behavior such as nonlinearity. This consideration makes the piecewise isometric dynamics the best vehicle to study and understand the singularity.

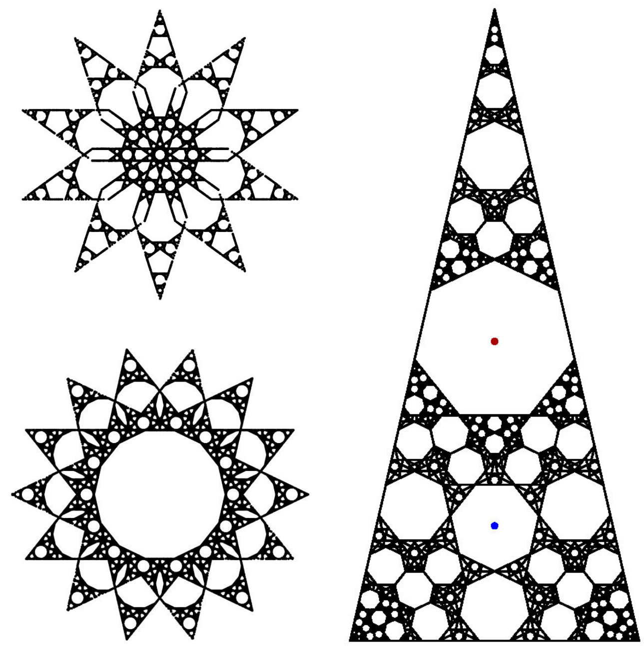

Fig. I.1. Selected Examples of the Singular Sets and the Exceptional Sets of a Class of Bounded Invertible Planar Piecewise Isometric Dynamical Systems

The purpose of the present research is to complete the characterization and the classification of the singularities of bounded invertible planar piecewise isometric dynamical systems, which had been initiated by the author through [22]. [22] classified the singularities of bounded invertible planar piecewise isometric systems as removable, sliding, and shuffling singularities, based upon their geometrical traits. The importance of this classification is best exmplified by the connection between the geometrical traits of the singularities and the dynamical properties of the system. As described in [20] and [21], as well as in [22], removable and shuffling singularities do not contribute toward Devaney-

Byungik Kahng, the corresponding author, is an assistant professor of mathematics in University of North Texas at Dallas, Dallas, TX 75241, U.S.A. (e-mail: byungik.kahng@unt.edu). He was supported, in part, by 2013 National Research Experience for Undergraduates Program (NREUP 2013), administered by Mathematical Association of America (MAA), funded by National Science Foundation (NSF).

Miguel Cuadros is an undergraduate student of University of North Texas at Dallas. (e-mail: miguel_cuadros@att.net). He was supported, in part, by 2013 National Research Experience for Undergraduates Program (NREUP 2013), administered by Mathematical Association of America (MAA), funded by National Science Foundation (NSF), under the supervision of the first author, Byungik Kahng.

Jonathan Sullivan is an undergraduate student of University of North Texas at Dallas. (e-mail: jonathan.k.sullivan@gmail.com). He was supported, in part, by 2013 National Research Experience for Undergraduates Program (NREUP 2013), administered by Mathematical Association of America (MAA), funded by National Science Foundation (NSF), under the supervision of the first author, Byungik Kahng.

The first part of this paper is an extended and retitled version of *Sliding, Shuffling and Self Shuffling Singularities of Bounded Invertible Planar Piecewise Isometric Dynamical Systems* (69501-184), which was presented in the 7th International Conference on Applied Mathematics, Simulation and Modeling, Cambridge, Massachusetts, U.S.A., January 30 – February 1, 2013 [23]. The second part, the numerical computation part, is a new addition that had not been presented in the afore-mentioned conference or anywhere else.

chaos, and thus the sliding singularities must be present whenever the dynamics is Devaney-chaotic. However, [22] came short of providing the complete distinction between sliding and shuffling singularities in simple terms, consequently, the afore-mentioned classification did not lead to the complete trichotomy. [22] got around the difficulty using the term, "non-shuffling sliding singularity," or "essential singularity," whenever the need arose.

This paper addresses this issue by proposing and proving a practical distinction between the sliding and shuffling singularities in simple terms. The key is to investigate and characterize the "self shuffling behavior," which will be elaborated in Theorem III.1.

Moreover, the "practical distinction" mentioned in the previous paragraph allows us to study the properties of the sliding singularities through a simple interval exchange dynamics, at least for a certain class of piecewise isometric systems. As a first step toward this line of research, we calculate the sliding ratios of a number of invertible planar piecewise isometries. These results are presented in Section IV and Section V.

II. Definitions and Preparations

Piecewise isometric dynamical systems can be defined in a number of ways. This paper follows the definitions and the terminologies of the author's earlier article, [22].

Definition II.1 (Piecewise Isometry). *Let $\{P_1, \cdots, P_n\}$ be a collection of mutually disjoint connected open regions in $\mathbb{R}^2$ with piecewise smooth boundary, and let $M = \bigcup_{i=1}^n \bar{P}_i$. A multiple-valued map $f : M \to \mathbb{R}^2$ is called a* **piecewise isometry** *subordinate to $\{P_1, \cdots, P_n\}$, if there exist isometries $f_i : \bar{P}_i \to \mathbb{R}^2$, $i \in \{1, \cdots, n\}$ such that $f(x) = \{f_i(x) : x \in \bar{P}_i\}$. Here, each P_i and f_i are called an* **atom** *and an* **isometric component** *of f, respectively. We say f is* **bounded**, *if each P_i is bounded. We say f is a* **polygon exchange**, *if each P_i is polygonal. We say f is a* **piecewise rotation**, *if each $f_i : \bar{P}_i \to \mathbb{R}^2$ is a rotation. Finally, we say f is* **invertible**, *if $f(P_i) \cap f(P_j) = \emptyset$ whenever $i \neq j$.*

Because $\{P_1, \cdots, P_n\}$ is mutually disjoint family of open sets, we must have $f(x) = f_i(x)$ if $x \in P_i$. Consequently, $f(x)$ can be multiple-valued only if x belong to a common boundary edge of some atoms P_i and P_j, that is, $x \in \partial P_i \cap \partial P_j$. Under the iteration of f, we can define the singularity structure of f as follows.

Definition II.2 (Singular Set and Exceptional Set). *Let $\{P_1, \cdots, P_n\}$, $\{f_1, \cdots, f_n\}$ and M be as in Definition II.1. Suppose that $f : M \to M$ is an invertible piecewise isometry subordinate to $\{P_1, \cdots, P_n\}$, with the isometric components $\{f_1, \cdots, f_n\}$. Let*

$$\Sigma^+ = \{x \in M : \ f \text{ is multiple-valued at } x\},$$
$$\Sigma^- = \{x \in M : \ f^{-1} \text{ is multiple-valued at } x\}.$$

We call the set, $\Sigma = \bigcup_{k=0}^{\infty} \left(f^k(\Sigma^+) \cup f^{-k}(\Sigma^-)\right)$, the **singular set** *of f. We call its closure $\bar{\Sigma}$, the* **exceptional set**.

Figure I.1 illustrates some example of the singularity structure of bounded invertible planar piecewise isometric systems. The black parts of the figures represent the exceptional sets. The singular sets are countable unions of curve segments, and thus has the 2-dimensional measure 0.

We need a couple more preparations before presenting the classification of the singularities.

Definition II.3 (Cutting Singularity). *Suppose that $\{P_1, \cdots, P_n\}$, $\{f_1, \cdots, f_n\}$, M and f are as in Definition II.2. We say f has the* **cutting singularity** *on a curve (segment) $S_{ij} = \partial P_i \cap \partial P_j$, if $\mu_1 \left(f_i(S_{ij}) \cap f_j(S_{ij})\right) = 0$, where μ_1 stands for the length. We say a curve (segment) $S \subset \Sigma^+$ is a* **cutting singularity** *of f, if it is a union of finitely many such S_{ij}'s.*

Definition II.4 (Isometric Continuation). *Suppose that $\{P_1, \cdots, P_n\}$, $\{f_1, \cdots, f_n\}$, M and f are as in Definition II.2. Suppose further that f has the cutting singularity on $S_{ij} = \partial P_i \cap \partial P_j$. Let $\equiv$ be the equivalence relation in M, which we will call the* **patch-up identification**, *given as follows.*

$$p \equiv q \Longleftrightarrow \begin{cases} \text{either} & (1)\ \ p = q; \\ \text{or} & (2)\ \ p = f_i(x) \text{ and } q = f_j(x), \\ & \quad\ \text{for some } x \in S_{ij}; \\ \text{or} & (3)\ \ p = f_j(x) \text{ and } q = f_i(x), \\ & \quad\ \text{for some } x \in S_{ij}. \end{cases}$$

Let us call the quotient map $\tilde{f} : \tilde{M} \to \tilde{M}$ of $f : M \to M$ in the quotient space $\tilde{M} = M/\equiv$, the **isometric continuation** *of f.*

Some singularities disappear as we take the patch-up identification and the isometric continuation. Such singularity is referred to **removable**. In general, an isometric continuation merely *postpones* the inevitable singularity. Repeated applications of the isometric continuation allow us to postpone the singularity finitely many times, but not indefinitely. Nonetheless, the idea of such postponement plays the key role in the proof of our main theorem, Theorem III.1.

In general, a non-removable singularity belongs to either one or both of the following classes. See [22] for detail.

Definition II.5 (Sliding Singularity). *Suppose that $\{P_1, \cdots, P_n\}$, $\{f_1, \cdots, f_n\}$, M and f are as in Definition II.2. We say f has the* **sliding singularity** *on a segment $S_{ij} = \partial P_i \cap \partial P_j$, if $\tilde{f}^k \circ f_i(S_{ij})$* **partly aligns** *with $\tilde{f}^l \circ f_j(S_{ij})$, for some isometric continuations $\tilde{f}^k$ and $\tilde{f}^l$, where $k, l \in \{0, 1, 2, \cdots\}$. That is, $\tilde{f}^k \circ f_i(S_{ij}) \cap \tilde{f}^l \circ f_j(S_{ij})$ is a curve segment with positive arc-length, but $\tilde{f}^k \circ f_i \neq \tilde{f}^l \circ f_j$ on $S_{ij} \subset \tilde{M}$.*

Definition II.6 (Shuffling Singularity). *Suppose that $\{P_1, \cdots, P_n\}$, $\{f_1, \cdots, f_n\}$, M and f are as in Definition II.2. We say f has the* **shuffling singularity** *on a segment $S_1 \subset \partial P_{i_1} \cap \partial P_{j_1}$, if there are a finite number of segments $S_k \subset \partial P_{i_k} \cap \partial P_{j_k}$, $k \in \{1, 2, \cdots, r\}$ and a positive integer $m \in \mathbb{Z}^+$ that satisfy the following conditions.*

(1) *For every S_k, $k \in \{1, \cdots, r\}$, there exists a certain S_l, $l \in \{1, \cdots, r\}$ such that $\tilde{f}^m \circ f_{i_k}(S_k) = \tilde{f}^m \circ f_{j_l}(S_l)$, upon taking appropriate branches of the isometric continuation $\tilde{f}^m$.*

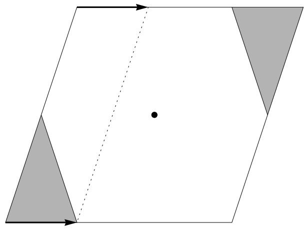

Fig. II.1. Before Iteration.

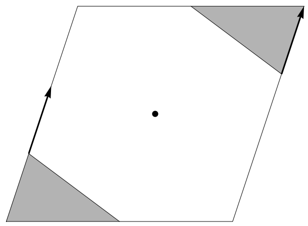

Fig. II.2. After Iteration.

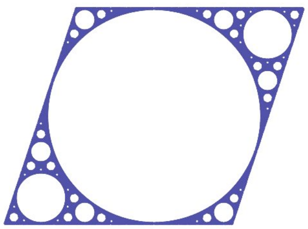

Fig. II.3. $\cos\theta = 1.25$.

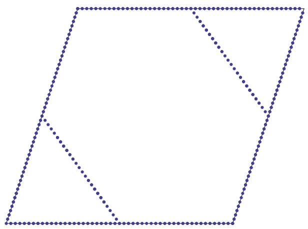

Fig. II.4. $\cos\theta = \cos(\pi/3) = 1/2$.

(2) $\mu_1(S_k \cap S_l) = 0$, *if* $k \neq l$. *That is, the intersection* $S_k \cap S_l$ *has length 0.*

(3) *Each* S_k *is the maximal segment with respect to the inclusion that satisfies (1) and (2).*

Figure II.1 and Figure II.2 depict one of the simplest examples of the sliding singularity. They visualize the sliding of the arrows as the slanted boundary edges get patched-up and identified. The resulting singularity structure is illustrated in Figure II.3. The intricate singularity does not always develop, as exemplified by Figure II.4. In some case, the singularity disappears, as depicted by Figure II.5 and Figure II.6, and thus the singularity structure does not develop at all.

The shuffling singularities, on the other hand, are visualized by Figure II.7 and Figure II.8. In this case, the singularity structure (Figure II.9 and Figure II.10) is notably different from that of the sliding singularity (Figure II.3).

III. Main Result

One of the most important features of the classification of the singularities discussed in the previous section is that the shuffling singularities are non-chaotic [22]. That is, the shuffling singularities do not generate the sensitive dependence upon the initial condition. In other words, if a bounded invertible planar piecewise isometric dynamical system is Devaney-chaotic in an appropriate invariant set, then

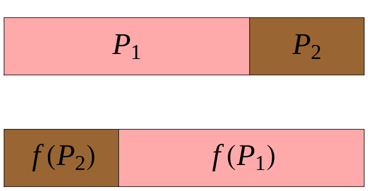

Fig. II.5. $M = \bar{P}_1 \cup \bar{P}_2$.

Fig. II.6. $\tilde{M}$. After Patch-up.

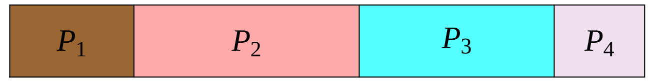

Fig. II.7. $M = \bar{P}_1 \cup \bar{P}_2 \cup \bar{P}_3 \cup \bar{P}_4$. Before Iteration.

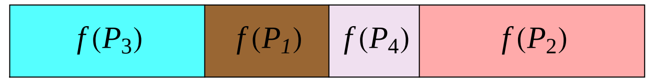

Fig. II.8. $M = f(\bar{P}_1) \cup f(\bar{P}_2) \cup f(\bar{P}_3) \cup f(\bar{P}_4)$. After Iteration.

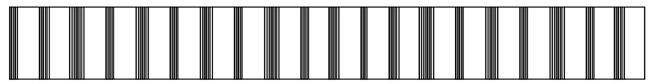

Fig. II.9. $\Sigma_{50} = \bigcup_{k=0}^{50} (f^k(\Sigma^+) \cup f^{-k}(\Sigma^-))$. After 50 Iterations.

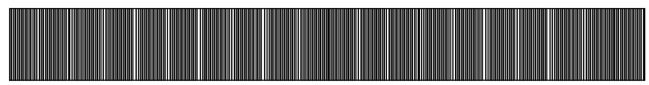

Fig. II.10. $\Sigma_{150} = \bigcup_{k=0}^{150} (f^k(\Sigma^+) \cup f^{-k}(\Sigma^-))$. After 150 Iterations.

there must exist some *non-shuffling sliding singularity* that generates the sensitive dependence upon the initial condition.

In practice, however, the "non-shuffling sliding singularity" is very difficult to deal with. Its main problem is the lack of clear distinction between the sliding and shuffling singularities. That is, there can be singularities that are both sliding and shuffling, which we call, **self-shuffling**. When dealing with Devaney-chaos, one must exclude such singularities, because all shuffling singularities are non-chaotic [22]. The main result of this paper is a simple criterion that tests whether a given sliding singularity is indeed non-shuffling.

Theorem III.1 (Self Shuffling Test)**.** *Let* $\{P_1, \cdots, P_n\}$, M, f *and* S_{ij} *be as in Definition II.5. Furthermore, suppose that* f *is a bounded piecewise isometry given by either a uniform rotation, that is, all* f_i*'s have the same rotational component and differ only by translations. Then the sliding singularity* S_{ij} *is non-shuffling if*

$$\frac{\mu_1\left(\tilde{f}^k \circ f_i(S_{ij}) \cap \tilde{f}^k \circ f_j(S_{ij})\right)}{\mu_1(S_{ij})} \notin \mathbb{Q}. \tag{III.1}$$

That is, S_{ij} *is non-shuffling, if the ratio between the length of overlap and the original length, which we call the* **sliding ratio***, is irrational.*

The technical part of the proof of Theorem III.1 depends heavily upon some results of [22]. For easier reading, we re-state the most critical parts here as follows.

Definition III.2 (Conjugate Points [22])**.** *Let* $\{P_1, \cdots, P_n\}$, $\{f_1, \cdots, f_n\}$, M *and* f *be as in Definition II.2. Also, let* $S_1 \subset \partial P_{i_1} \cap \partial P_{j_1}, \cdots, S_r \subset \partial P_{i_r} \cap \partial P_{j_r}$ *and* $m \in \mathbb{N}$ *be as in Definition II.6. We say* $x_k \in P_{i_k}$ *and* $x_l \in P_{i_l}$ *are* **conjugate** *of each other if* x_l *is positioned in the same geometrical location from* S_l *as* x_k *is from* S_k*, as illustrated in Figure III.1. The*

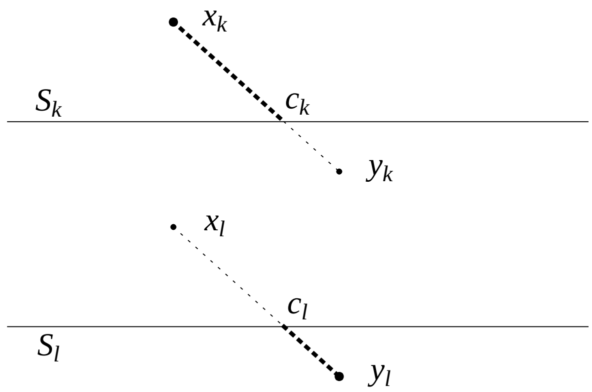

Fig. III.1. Conjugate Points.

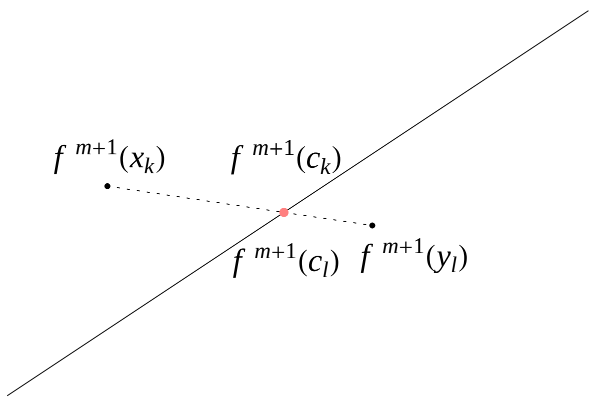

Fig. III.2. Shuffling Singularity Theorem.

$$\mu_1(\overline{x_k y_k}) = \mu_1(\overline{x_l y_l}) = \mu_1(\overline{f^{m+1}(x_k) f^{m+1}(y_l)}).$$

conjugacy relation between y_k and y_l are defined similarly.

Theorem III.3 (Shuffling Singularity Theorem [22]). *Let $\{P_1, \cdots, P_n\}$, $\{f_1, \cdots, f_n\}$, M and f be as in Definition II.2. Let $S_1 \subset \partial P_{i_1} \cap \partial P_{j_1}, \cdots, S_r \subset \partial P_{i_r} \cap \partial P_{j_r}$ and $m \in \mathbb{N}$ be as in Definition II.6. Let x_k and y_k, $k \in \{1, \cdots, r\}$ be as in Definition III.2. Suppose further that each x_k and y_k are separated up to $m+1$ iterations only by S_k. That is, the line segment $\overline{x_k y_k}$ crosses $\bigcup_{l=0}^{m} f^{-l}(\Sigma^+)$ (Definition II.2) only once, and the crossing point, c_k, belong to S_k. Then, for every $k \in \{1, \cdots, r\}$, there exists a unique $l \in \{1, \cdots, r\}$ that satisfies the following conditions.*

(1) *$\tilde{f}^m \circ f_{i_k}(c_k) = \tilde{f}^m \circ f_{j_l}(c_l)$. That is, the two points merge to the same point after $m+1$ iterations, upon taking appropriate branches.*

(2) *The curve segment $\overline{f^{m+1}(x_k) f^{m+1}(y_l)}$ is a line segment that runs through the (common) point $\tilde{f}^m \circ f_{i_k}(c_k) = \tilde{f}^m \circ f_{j_l}(c_l)$.*

(3) *$\mu_1\left(\overline{x_k y_k}\right) = \mu_1\left(\overline{f^{m+1}(x_k) f^{m+1}(y_l)}\right)$. That is, the length of the line segment is preserved.*

See Figure III.1 and Figure III.2.

Proof. See [22]. □

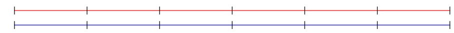

Fig. III.3. $S_{ij} = S_{ij}^1 \cup S_{ij}^2 \cup \cdots \cup S_{ij}^n$. For Rational Sliding Ratio.

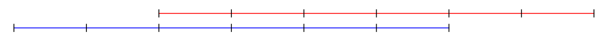

Fig. III.4. $\tilde{f}^k \circ f_i(S_{ij})$ and $\tilde{f}^k \circ f_j(S_{ij})$. For Rational Sliding Ratio.

The Proof of Theorem III.1. Because f is given by a uniform rotation, any orbit of any segment of S_{ij} must have the same slope. Therefore, if some segments of $\tilde{f}^k \circ f_i(S_{ij})$ and $\tilde{f}^l \circ f_j(S_{ij})$ align each other, we must have $k = l$. Examples in Section IV illustrates this phenomenon. Also, see Section V for an example of a non-uniform rotation, leading up to $k \neq l$.

When the fraction in the condition (III.1) is irrational, then the finite subdivision depicted in Figure III.3 and Figure III.4 is impossible. More specifically, a point in S_{ij} is shifted by an irrational amount as the iterate of S_{ij} overlaps itself. Because the repetition of an irrational shifting is aperiodic, the orbit of the repetition will include an infinitely many points. This contradicts Theorem III.3, which implies that the shuffling singularity generates only finitely many such points (conjugate points of Definition III.2). See [22] for more detail on the conjugate points of the shuffling singularity. See also, [20] and [21] for the role of the conjugacy toward Devaney-chaos. □

The practical use of the condition (III.1) of Theorem III.1 will be discussed in the following two subsections.

IV. Applications of Theorem III.1

EVEN though the condition (III.1) of Theorem III.1 does help completing the classification of the singularities of a class of bounded invertible planar piecewise isometric dynamical systems, it is not always easy to apply the condition (III.1) directly and calculate the sliding ratio. In some cases, however, it is possible to calculate the sliding ratio explicitly. One of the simplest non-trivial case is the iterative dynamics of Symmetric Uniform Piecewise Elliptic Rotation maps (SUPER maps) [14], [15], [16], [17], [18], which were developed from modeling digital signal processing and also kicked oscillation. The orbit structure and the singularity structure of this class of dynamics are exemplified in Figure IV.1.

The general definition of a SUPER map is as follows.

$$F_\theta : \begin{pmatrix} x \\ y \end{pmatrix} \mapsto \begin{pmatrix} 0 & -1 \\ 1 & 2\cos\theta \end{pmatrix} \begin{pmatrix} x \\ y \end{pmatrix} + \begin{pmatrix} 1 \\ -\cos\theta + \sigma \end{pmatrix}, \quad \text{(IV.1)}$$

where $0 < \theta < \pi/2$, and $\sigma = 0, 1$ or -1 such that

$$0 \leq x + 2y\cos\theta - \cos\theta + \sigma \leq 1. \quad \text{(IV.2)}$$

It is easy to see that the condition (IV.2) ensures that $F_\theta : [0,1]^2 \to [0,1]^2$, and the map is double-valued at (x, y) when and only when $x + 2y\cos\theta - \cos\theta = 0$ or 1, thus creating the cutting-singularity. See, for instance, [14] for more detail. In fact, it is possible to consider the rotation angle beyond $0 < \theta < \pi/2$, but the singularity structure for those cases turn out to be identical to those of $0 < \theta < \pi/2$ case due to the symmetry and periodicity of cosine function. For this reason,

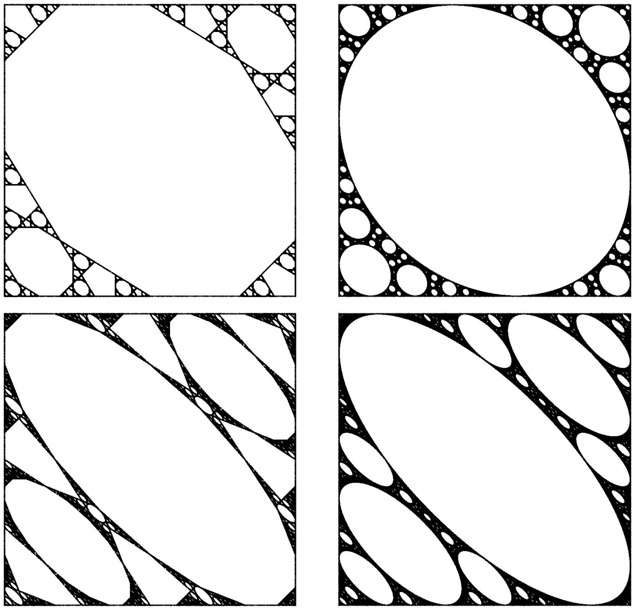

Fig. IV.1. Selected Examples of the Singularity Structure of Symmetric Uniform Piecewise Elliptic Rotation Maps

we generally consider only $0 < \theta < \pi/2$ case. See [14], if for more detail is needed.

Although a SUPER map is not exactly a piecewise isometry, it can be regarded as one by tilting the unit square in an appropriate angle as in Figure II.1 – Figure II.4 [14]. Furthermore, upon taking the standard boundary-identification to lift up the unit square $[0,1]^2$ to the 2-torus $\mathbb{T}^2$, the cutting-singularity of a SUPER map becomes a sliding singularity. Figure II.1 and Figure II.2 illustrate the sliding behavior of a SUPER map under an appropriate tilting. It is not difficult to see that the afore-mentioned tilting and the 2-torus representation of a SUPER map corresponds to the isometric continuation. The detail is left to the readers. Also, see [14] for more detail.

The sliding ratio of a SUPER map can be calculated by comparing the relative positions of the arrows in Figure II.1 and Figure II.2. Here, the k value of the condition (III.1) is 1. Because the starting points of the arrows are the lower left hand side corner and the upper left hand side corner of Figure II.1, they correspond to $(0,0)$ and $(0,1)$ in the unit square, respectively. From the straightforward matrix computation, we can easily see that the difference of the y-coordinates of $F_\theta(0,0)$ and that of $F_\theta(0,1)$ is $(2\cos\theta - \cos\theta) - (-\cos\theta)$ (mod 1), or $2\cos\theta$ (mod 1).

In general, the sliding ratio, $2\cos\theta$ (mod 1) is an irrational number. Therefore, as a result of Theorem III.1, the sliding singularity is not self-shuffling.

It becomes a rational number when and only when $\theta = \pi/3$. Incidentally, this case is the only possible case when the singularity disappears, as depicted in Figure II.4. In other words, our main result, Theorem III.1 perfectly fits the known results, as far as the dynamics of SUPER maps are concerned.

The sliding ratios of SUPER maps are not the only numerical evidence that supports the validity of Theorem III.1. The condition (III.1) can be applied to another well known class

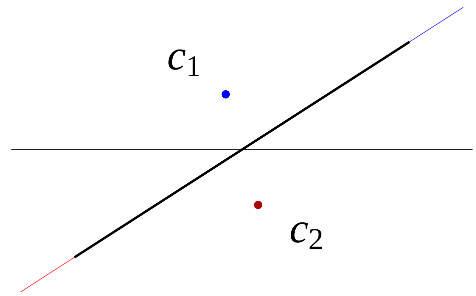

Fig. IV.2. $\mathbb{R}^2 = \bar{P}_1 \cup \bar{P}_2$.

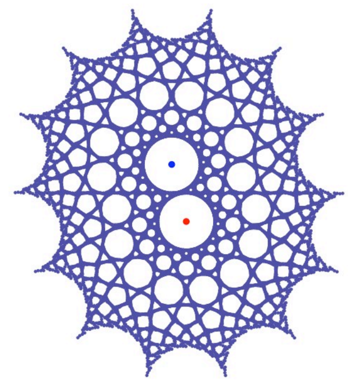

Fig. IV.3. A Part of $\bar{\Sigma}$ for $\theta = \pi/8$.

of piecewise isometries, which are commonly known Goetz maps. Figure IV.2 and Figure IV.3 illustrate the dynamics and the singularity structure of an example of an invertible Goetz map.

The class of Goetz maps that we are particularly interested in is those defined by

$$f(x,y) = \begin{cases} f_1(x,y), & \text{if } y \geq 0, \\ f_2(x,y), & \text{if } y \leq 0, \end{cases} \qquad \text{(IV.3)}$$

where

$$\begin{cases} f_1(x,y) = R_\theta(x-p_1, y-q_1) + (p_1,q_1), \\ f_2(x,y) = R_\theta(x-p_2, y-q_2) + (p_2,q_2), \end{cases}$$

$$\begin{cases} (p_1,q_1) = (-\sin(\theta/2), \cos(\theta/2)), \\ (p_2,q_2) = (\sin(\theta/2), -\cos(\theta/2)), \end{cases}$$

and R_θ is the rotation by the angle θ about $(0,0)$ such that $0 < \theta < \pi/2$. Again, the restriction, $0 < \theta < \pi/2$ is there to eliminate the redundancy. Note that map f is defined by the equality (IV.3) is multiple valued on the x-axis, or $\{(x,y) \in \mathbb{R}^2 : y = 0\}$, of $\mathbb{R}^2$, thus creating the singularity. The nature of this singularity is sliding, as illustrated in Figure IV.2. In fact, Figure IV.2 and Figure IV.3 illustrate the dynamics and the singularity structure of the Goetz map defined as above for $\theta = \pi/8$.

Although the Goetz maps defined as above are not bounded, we can still calculate the sliding ratio through the straightforward matrix computation to the condition condition (III.1). We get, $||f_1(0,0) - f_2(0,0)||$ (mod 1), which can be simplified to

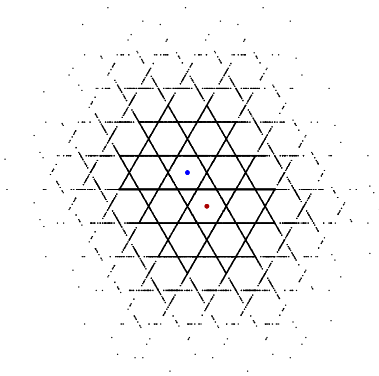

Fig. IV.4. A Part of $\bar{\Sigma}$ for $\theta = \pi/3$.

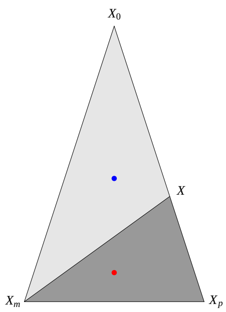

Fig. V.1. $\bar{P}_i$'s.

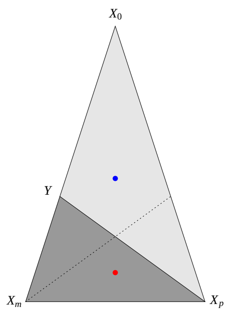

Fig. V.2. $\overline{f_i(P_i)}$'s.

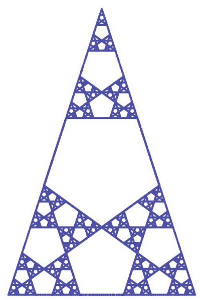

Fig. V.3. $\bar{\Sigma}$.

$4\sin(\theta/2)$ (mod 1). Again, the only way to get the rational sliding ratio is to set $\theta = \pi/3$, and that is the only possible case for which the singularity disappears altogether. Figure IV.4 illustrates this phenomenon. The grid is formed as the orbit of the x-axis, but it does not contain any essential singularity.

V. Further Discussion

Although our main theorem, Theorem III.1 was stated under the restriction of "uniform rotation", it appears that some kind of extension is possible, at least for a certain type of systems. Figure V.1 – Figure V.3 illustrate the dynamics and the singularity structure of a bounded invertible piecewise isometric system given by two rotations in an isosceles triangle with the top angle $\theta = \pi/5$. The centers of the rotations are depicted as the dots in the light gray and dark gray triangles in Figure V.1 (before-picture) and Figure V.2 (after-picture). The light gray triangle is rotated by $-4\pi/5$ while the dark gray triangle is rotated by $4\pi/5$, with respect to their respective centers of the rotations. This map is similar to the class of Goetz maps introduced in the previous section, in that the piecewise isometry is generated by two rotations. In this case, however, the rotation angles are different and the piecewise isometry is bounded. This map was studied first by Arek Goetz in [9], but the figures in this article came from [22]. See, also, [31] for further development of this map.

The computation of the sliding ratio for this case depends heavily on the isometric continuation process discussed in [22]. For easier reading, we will review the process briefly here. See [22] for more detail.

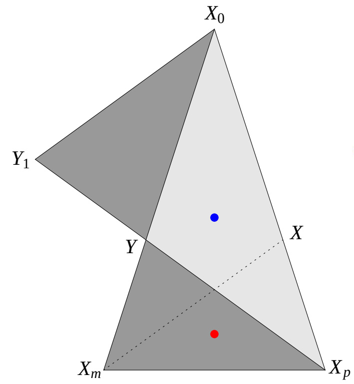

Fig. V.4. Patch-up #1.

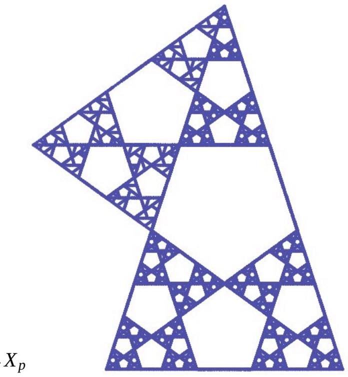

Fig. V.5. Patch-up #1.

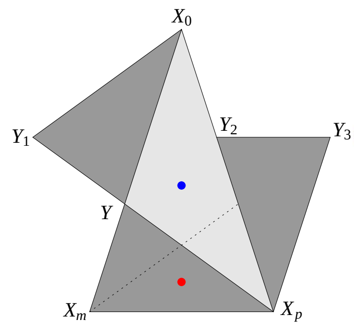

Fig. V.6. Patch-up #2.

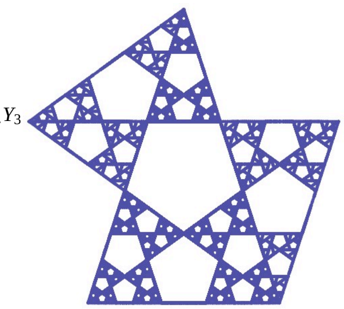

Fig. V.7. Patch-up #2.

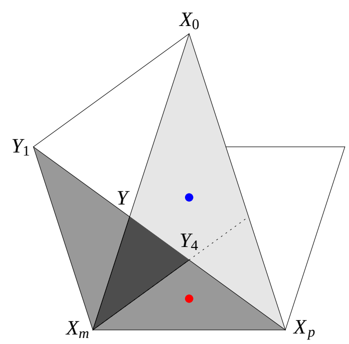

Fig. V.8. Patch-up #3.

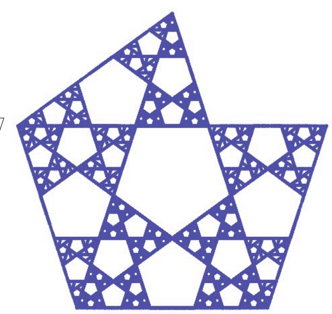

Fig. V.9. Patch-up #3.

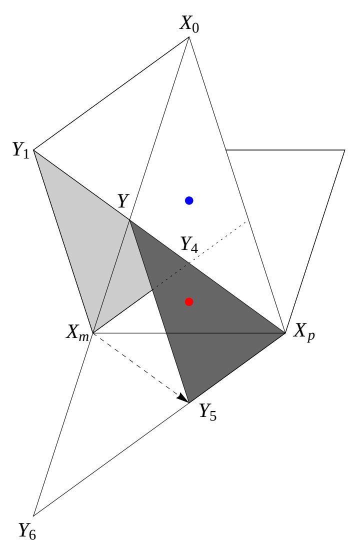

Fig. V.10. Sliding.

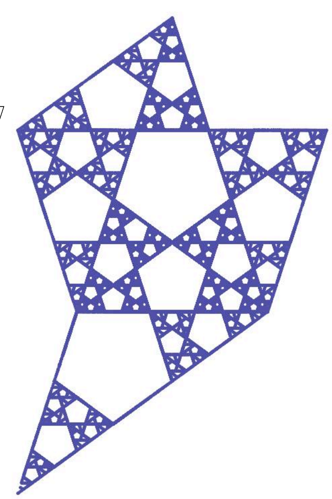

Fig. V.11. Sliding.

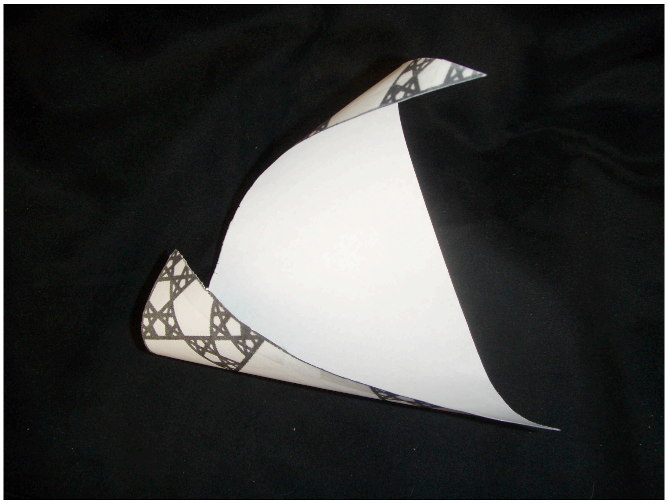

Fig. V.12. Patch-up Preparation.

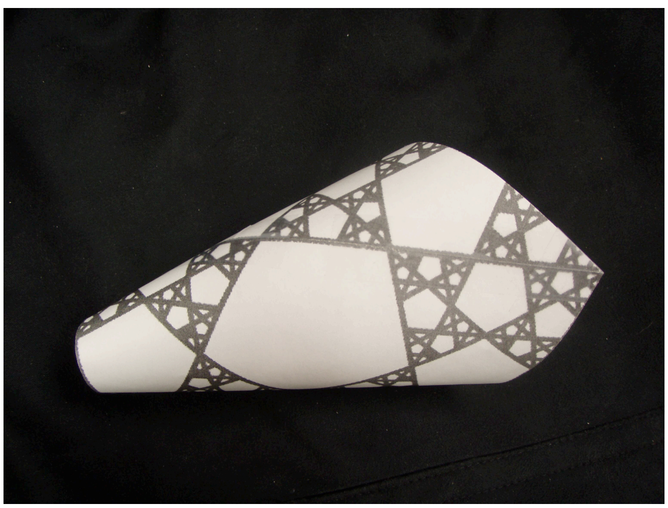

Fig. V.13. Patch-up Complete.

Figure V.4 – Figure V.9 depict the patch up identification and the isometric continuation of the orbit of the light triangle up to three iterations. First, by patching up the edges $\overline{X_0Y}$ of Figure V.4 and $\overline{X_pX_m}$, we identify the dark gray triangular regions $\triangle(X_0YY_1)$ and $\triangle(X_pX_mY)$. This patch-up identification and the ensuing isometric continuation are visualized in Figure V.12 and Figure V.13. Figure V.12 depicts the intermediate process of bending the domain to identify the edges $\overline{X_0Y}$ and $\overline{X_pX_m}$ of Figure V.4. When the patch-up is complete, $\triangle(X_0YY_1)$ covers $\triangle(X_0YY_1)$ from below, as Figure V.13 shows. As a consequence, the discontinuity temporarily disappears, and our piecewise isometry becomes continuous in $\widetilde{M}$ of Figure V.13.

Figure V.6 and Figure V.7 depict the repetition of the same process, starting from the triangular region, $\triangle(X_pY_1X_0)$, which is essentially a rotated copy of $\triangle(X_0X_mX_p)$ of Figure V.1. At the third iteration, the process must stop because the singular edge came out of ∂M and aligned itself with another singular edge, as Figure V.8 and Figure V.9 indicate. Finally, Figure V.10 and Figure V.11 illustrate the amount of sliding. For more detailed description of each step, see [22].

As justified by Figure V.4 – Figure V.11, we can conduct a straightforward matrix computation to find out the sliding ratio,

$$\text{Ratio} = \mu_1(\overline{Y_1Y})/\mu_1(\overline{YX_p}).$$

Using a computer algebra system, we can conduct the matrix computations to calculate the sliding ratio precisely. It turns out that the ratio is, $(\sqrt{5}-1)/2$. The same value as $2\cos(\pi/5)-1$ and $2\cos(2\pi/5)$, which are the sliding ratios of the SUPER maps of the rotation angles $\theta = \pi/5$ and $\theta = 2\pi/5$, respectively.

VI. Conclusion

The main result of this paper is Theorem III.1, which presents a condition far more practical than those of Definition II.5 and Definition II.6. And then, we verified its usefulness through some explicit calculations for selected examples of well known piecewise isometric systems.

The computations we did in Section IV revealed little but the usefulness of the practical condition (III.1) of Theorem III.1 over the conditions of Definition II.5 and Definition II.6. The work we put in to understand the dynamics of the triangle map in Section V, on the other hand, appears to suggest something extra. It appears that Theorem III.1 can be extended beyond the uniform rotation condition. For the moment, we do not have clear idea how to proceed in further developing Theorem III.1. However, the authors cautiously conjecture that the majority (if not all) of Theorem III.1 will hold also for dual rotation or more complicated classes of piecewise isometric dynamical systems. For now, we leave this topic as a problem for a future research.

References

[1] R. Adler, B. Kitchens, and C. Tresser, *Dynamics of non-ergodic piecewise affine maps of the torus*, Ergo. The. & Dynam. Sys., 21 (2001), pp. 959–999.

[2] P. Ashwin, *Non-smooth invariant circles in digital overflow oscillations*, in Proceedings of the 4th International Workshop on Nonlinear Dynamics and Electronic Systems, pp. 417–422.

[3] ———, *Elliptic behavior in the sawtooth standard map*, Phys. Lett. A, 232 (1997), pp. 409–416.

[4] P. Ashwin, W. Chambers, and G. Petrov, *Lossless digital filter overflow oscillations: approximation of invariant fractals*, Int. J. Bifur. Chaos Appl. Sci. Eng., 7 (1997), pp. 2603–2610.

[5] L. O. Chua and T. Lin, *Chaos in digital filters*, IEEE Trans. Circuits and Systems, CAS-35 (1988), pp. 646–658.

[6] A. C. Davis, *Nonlinear oscillations and chaos from digital filter overflow*, Phil. Trans. Royal Soc. Lond., A-353 (1995), pp. 85–99.

[7] Z. Galias and M. Ogorzalek, *Bifurcation phenomena in second order digital filter with saturation type adder overflow characteristic*, IEEE Trans. Circ. Sys., 37 (1990), pp. 1068–1070.

[8] A. Goetz, *Piecewise isometries - an emerging area of dynamical systems*, in Trends in Mathematics: Fractals in Graz 2001, P. Grabner and W. Woess, eds., pp. 135–144.

[9] ———, *Dynamics of piecewise isometries*, Illinois J. Math., 44 (2000), pp. 465–478.

[10] E. Gutkin and N. Simanyi, *Dual polygonal billiards and necklace dynamics*, Commun. Math. Phys., 143 (1992), pp. 431–449.

[11] B. Kahng, *The approximate control problems of the maximal invariant sets of nonlinear discrete-time disturbed control dynamical systems: an algorithmic approach*, in Proceedings of the 4th International Conference on Control, Automation and Systems, pp. 1513–1518.

[12] ———, *The invariant set theory of multiple valued iterative dynamical systems*, in Proceedings of the 7th WSEAS International Conference on SYSTEM SCIENCE and SIMULATION in ENGINEERING (ICOSSSE '08), pp. 19–24.
[13] ———, *Positive invariance of multiple valued iterative dynamical systems in disturbed control models*, in Proceedings of the 17th IEEE Mediterranean Conference on Control and Automation, pp. 664–668.
[14] ———, *Dynamics of symplectic piecewise affine eliptic rotations maps on tori*, Ph. D. Thesis, University of Ilinois at Urbana-Champaign, 2000.
[15] ———, *Dynamics of symplectic piecewise affine eliptic rotations maps on tori*, Ergod. Th. & Dynam. Sys., 22 (2002), pp. 483–505.
[16] ———, *Dynamics of kaleidoscopic maps*, Adv. Math., 185 (2004), pp. 178–205.
[17] ———, *The invariant fractals of symmetric piecewise affine elliptic dynamics*, Proc. Sympo. Pure Math., Amer. Math. Soc., 72 (2004), pp. 375–389.
[18] ———, *The unique ergodic measure of the symmetric piecewise toral isometry of rotation angle $\theta = \pi/5$ is the hausdorff measure of its singular set*, Dynam. Sys., 19 (2004), pp. 245–264.
[19] ———, *Maximal invariant sets of multiple valued iterative dynamics in disturbed control systems*, Int. J. Circ. Sys. and Signal Proc., 2 (2008), pp. 113–120.
[20] ———, *On Devaney's Definition of Chaos for Discontinuous Dynamical Systems*, in Proc. 15th Amer. Conf. on Appl. Math., Houston, TX, U.S.A., 2009, pp. 89–94.
[21] ———, *Redifining chaos: Devaney-chaos for piecewise isometric dynamical systems*, International Journal of Mathematical Models and Methods in Applied Sciences, 4 (2009), pp. 317–326.
[22] ———, *Singularities of 2-dimensional invertible piecewise isometric dynamics*, Chaos, 19 (2009), p. 023115.
[23] ———, *Sliding, Shuffling and Self Shuffling Singularities of Bounded Invertible Planar Piecewise Isometric Dynamical Systems*, in Proc. 7th Int. Conf. on Applied Mathematics, Simulation and Modeling, Cambridge, MA, U.S.A., 2013, pp. 118–123.
[24] L. KOCAREV, C. W. WU, AND L. O. CHUA, *Complex behavior in digital filters with overflow nonlinearity: analytical results*, IEEE Trans. Circuits and Systems - II, 43 (1996), pp. 234–246.
[25] T. LIN AND L. O. CHUA, *A new class of pseudo-random generators based on chaos in digital filters*, Int. J. Cir. Th. Appl., 21 (1993), pp. 473–480.
[26] J. H. LOWENSTEIN, *Aperiodic orbits of piecewise rational rotations of convex polygons with recursive tiling*, Dynam. Sys., 22 (2007), pp. 25–63.
[27] J. H. LOWENSTEIN, K. L. KUPTSOV, AND F. VIVALDI, *Recursive tiling and geometry of piecewise rotations by $\pi/7$*, Nonlinearity, 17 (2004), pp. 371–396.
[28] J. H. LOWENSTEIN, G. POGGIASPALLA, AND F. VIVALDI, *Sticky orbits in a kicked-oscillator model*, Dynam. Sys., 20 (2005), pp. 413–451.
[29] M. OGORZALEK, *Chaos and Complexity in Nonlinear Electronic Circuits*, vol. 22 of Series on Nonlinear Science Monographs and Treatises A, World Scientific, Singapore, 1st ed., 1997.
[30] S. TABACHNIKOV, *On the dual billiard problem*, Adv. Math., 115 (1995), pp. 221–249.
[31] M. TROVATI AND P. ASHWIN, *Tangency properties of a pentagonal tiling generated by a piecewise isometry*, Chaos, 17 (2007), p. 043129.